

# Magnetic Resonance Contrast Agents from Viral Capsid Shells: A Comparison of Exterior and Interior Cargo Strategies

Jacob M. Hooker,<sup>†</sup> Ankona Datta,<sup>†</sup> Mauro Botta,<sup>‡</sup> Kenneth N. Raymond,<sup>†</sup> and Matthew B. Francis<sup>\*,†,§</sup>

*Department of Chemistry, University of California, Berkeley, California 94720-1460, Dipartimento di Scienze dell' Ambiente e della Vita, Università del Piemonte Orientale "A. Avogadro", Via Bellini 25/G, Alessandria, Italy, and Materials Sciences Division, Lawrence Berkeley National Laboratory, Berkeley, California 94720*

Received March 4, 2007; Revised Manuscript Received May 23, 2007

## ABSTRACT

Two high-relaxivity nanoscale magnetic resonance contrast agents have been built using bacteriophage MS2 as a biomolecular scaffold. Protein capsid shells were functionalized on either the exterior or interior surface to display multiple copies of an aldehyde functional group. Subsequently, ~90 heteropodal bis(hydroxypyridonate)terephthalamide ligands were attached to these sites through oxime condensation reactions. Upon complexation with Gd<sup>3+</sup>, contrast agents with ionic relaxivities of up to 41.6 mM<sup>-1</sup> s<sup>-1</sup> (30 MHz, 25 °C) and total molecular relaxivities of up to 3900 mM<sup>-1</sup> s<sup>-1</sup> (30 MHz, 25 °C) were produced. Capsids sequestering the Gd-chelates on the interior surface (attached through tyrosine residues) not only provided higher relaxivities than their exterior functionalized counterparts (which relied on lysine modification) but also exhibited improved water solubility and capsid stability. The attachment functional cargo to the interior surface is envisioned to minimize its influences on biodistribution, yielding significant advantages for tissue targeting by additional groups attached to the capsid exterior.

The use of chemically modified viral capsids is an emerging technology for the development of high relaxivity magnetic resonance imaging (MRI) contrast agents.<sup>1–3</sup> This development parallels the use of other macromolecular constructs, including polymers,<sup>4–6</sup> dendrimers,<sup>7–9</sup> and liposomes,<sup>10</sup> that are designed to increase the rotational correlation time ( $\tau_R$ ) of a contrast agent and therefore enhance its relaxivity.<sup>11</sup> As an additional feature, the polyvalent nature of viral capsids allows for the attachment of multiple Gd<sup>3+</sup> complexes, thus increasing the overall molecular relaxivity of a single carrier. The first demonstration of these concepts capitalized on the inherent affinity of Gd<sup>3+</sup> for Ca<sup>2+</sup> binding sites present in the capsid of the cowpea chlorotic mottle virus (CCMV).<sup>1</sup> Although the Gd<sup>3+</sup> binding affinity ( $K_d = 31 \mu\text{M}$ ) was too low for use in a biological context, the remarkably high T<sub>1</sub> ionic relaxivity (>200 mM<sup>-1</sup> s<sup>-1</sup> at 61 MHz) has encouraged further development of viral-based contrast agents. A subsequent report addressed the low Gd<sup>3+</sup> binding affinity through the covalent attachment of a commercially available Magnevist isothiocyanate derivative (2-(4-isothiocyanato-

benzyl)-Gd-diethylenetriaminopentaacetic acid, Gd-DTPA-ITC) to the exterior surface of bacteriophage MS2.<sup>2</sup> The covalent attachment to MS2 provided a 3-fold T<sub>1</sub> relaxivity enhancement when compared to an unconjugated Gd-DTPA moiety, giving an ionic relaxivity of 14.0–16.9 mM<sup>-1</sup> s<sup>-1</sup> and a molecular relaxivity of up to 7200 mM<sup>-1</sup> s<sup>-1</sup> (at 64 MHz). The most recent report of MR contrast materials from virions accomplished the attachment of Gd-DOTA to the cowpea mosaic virus (CPMV) using a Cu-mediated azide–alkyne cycloaddition reaction.<sup>3</sup> This report also demonstrated that the RNA packaged within a virion can bind free lanthanide ions, including Gd<sup>3+</sup>. The combination of these methods resulted in CPMV particles with relaxivities at 64 MHz of up to 15.5 mM<sup>-1</sup> s<sup>-1</sup> (per Gd) and 4150 mM<sup>-1</sup> s<sup>-1</sup> (per particle).

A key advantage of virus-based biomedical agents is the ability to differentiate rigidly defined interior and exterior surfaces through chemoselective bioconjugation reactions.<sup>12,13</sup> With cargo sequestered on the interior surface of a viral capsid shell, the exterior surface remains available for the display of molecules that dictate biodistribution. With this masked payload strategy, it is further anticipated that the nature of the internal cargo will have minimal impact on receptor targeting of the agent. Indeed, several research groups have successfully modified the interior surface of viral

\* Corresponding author: francis@cchem.berkeley.edu.

<sup>†</sup> Department of Chemistry, University of California, Berkeley.

<sup>‡</sup> Dipartimento di Scienze dell' Ambiente e della Vita, Università del Piemonte Orientale "A. Avogadro".

<sup>§</sup> Materials Sciences Division, Lawrence Berkeley National Laboratory.

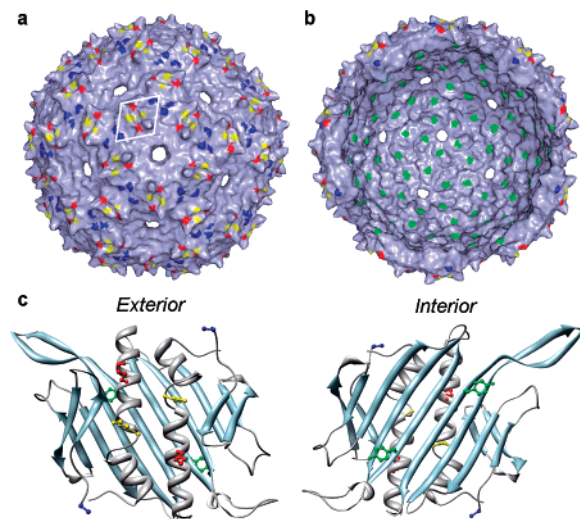


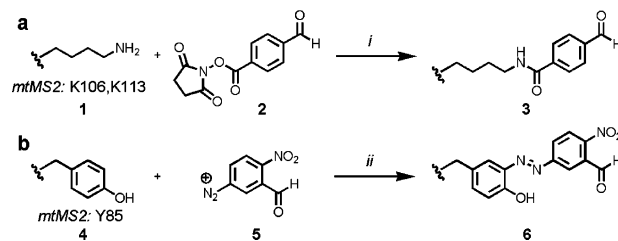
**Figure 1.** Crystal structure renderings of bacteriophage MS2 coat protein. (a) The exterior surface of MS2 displays lysine 106 (red), lysine 113 (yellow), and the N-terminus (blue) that are reactive toward NHS esters. A coat protein dimer is outlined in white. (b) The interior surface of MS2 displays tyrosine 85 (green) that is selectively reactive toward electron-deficient diazonium salts. (c) Ribbon structure renderings of an MS2 coat protein dimer with Lys106, Lys113, the N-terminus, and Tyr85 highlighted, showing the orientation of the reactive amino acid side chains.

capsid shells in order to display drug molecules,<sup>14</sup> fluorophores,<sup>15</sup> and organic functional groups.<sup>16</sup> For modified viral capsids to serve as MR contrast agents, however, it is critically important to weigh the advantages of internal placement against the factors affecting relaxivity, such as the transport of water through the capsid shell. To evaluate these effects, we have developed a modular synthetic strategy for the independent decoration of each surface of bacteriophage MS2 with high relaxivity contrast agents.

Bacteriophage MS2 was chosen as the scaffold for these studies due to several features, perhaps the most influential of which being the presence of 32 pores along the 5- and 3-fold symmetry axes.<sup>17</sup> We have previously shown that these 1.8 nm “holes” allow large organic molecules to access the interior surface, Figure 1.<sup>12</sup> In addition to permitting relatively large Gd<sup>3+</sup> chelating ligands to reach the capsid interior for covalent attachment, it was assumed that these pores would allow rapid water transport. Although after propagation the capsids contain a genome of single-stranded RNA, we have found that the nucleic acids can be completely removed under basic conditions.<sup>12</sup> The resulting “empty” MS2 (mtMS2) capsids are markedly stable toward acidic and alkaline buffers, organic cosolvents, and chemical manipulation.<sup>9,12,18</sup>

In terms of chemical synthesis, the interior and exterior surfaces of MS2 were targeted independently through the appropriate choice of reagents, Scheme 1. Exterior surface amines (Lys106, Lys113, and the N-terminus) or interior surface tyrosines (Tyr85) were first modified to display an aldehyde functional group (Scheme 1). As has been demonstrated previously, aldehydes are exceptionally useful functional groups for chemoselective biomolecule ligations.<sup>19–21</sup> Briefly, the attachment of an aldehyde to the exterior surface amines (**1**) was accomplished with NHS ester **2** in pH 9.0

**Scheme 1.** Orthogonal MS2 Bioconjugation Strategies for the Attachment of an Aldehyde Group to (a) the Exterior or (b) the Interior Surface<sup>a</sup>



<sup>a</sup> Conditions: (i) 250  $\mu$ M mtMS2 (based on monomer), 1 mM **2**, 100 mM NaH<sub>2</sub>PO<sub>4</sub> pH 9.0, 2 h. (ii) 150  $\mu$ M MS2, 1.5 mM **5**, 100 mM NaH<sub>2</sub>PO<sub>4</sub> pH 8.6, 4  $^{\circ}$ C, 30 min.

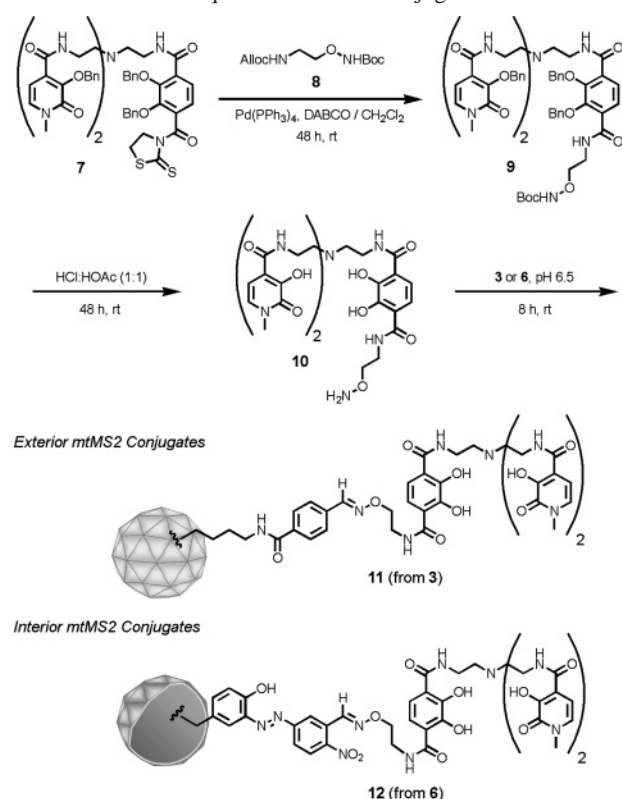
phosphate buffer, affording **3**. Alternatively, the attachment of an aldehyde group to the interior surface was accomplished through the reaction of Tyr85 (**4**) with highly electron deficient diazonium salt **5** (synthesized in six steps from *m*-nitrobenzaldehyde, see Supporting Information) to yield azo-conjugate **6**. The extent of conversion for these primary bioconjugation reactions, and therefore the amount of “payload” that could be introduced, was controlled through optimization of the reaction conditions and careful control of the stoichiometry. Coupling conversions were based on integration of electrospray ionization mass spectrometry (ESI-MS) peaks and corroborated by UV–vis spectroscopy.

In order to maximize the relaxivity of each Gd<sup>3+</sup> complex attached to the MS2 scaffold, we chose to attach hydroxy-pyridonate (HOPO)-based contrast agents.<sup>22</sup> It has been shown that contrast agents based on these (and similar) ligands have greater than 3-fold higher relaxivities and equivalent stabilities when compared to commercial agents. Crucial to the performance of these complexes is the fast water exchange that they exhibit, which can allow relaxivity enhancements of nearly 100-fold as additional parameters are optimized. In addition, the development of heteropodal bis(HOPO)-TAM (terephthalamide) complexes has allowed for the attachment of virtually any reactive functional group to the ligand via the terminal acid of the TAM moiety.<sup>23–25</sup>

A single bis(HOPO)-TAM reagent was synthesized to functionalize the two different surfaces of MS2 (Scheme 2). In addition to being efficient, this modular strategy also minimizes structural changes in the linker portion of the ligand that could affect the relaxivity of the macromolecular Gd chelates. An activated carboxylate of the TAM group (**7**) reacted with amine-alkoxyamine precursor **8** in the presence of palladium(0). Following global deprotection of **9** in 1:1 HCl/HOAc, aldehyde-reactive ligand **10** was coupled to either the outside (via **3**) or the inside (via **6**) of the MS2 capsids. The oxime condensation reactions proceeded quantitatively at pH 6.5 in under 12 h (as determined by ESI-MS, Figure 2), requiring only a slight excess of chelating ligand **10** (see Supporting Information for details).

For conjugate **11**, a significant solubility change occurred when placing the large hydrophobic ligands on the exterior surface. Capsids that averaged greater than one modification per monomer were found to precipitate at all protein

**Scheme 2.** Synthesis of Bis(HOPO)-TAM Alkoxyamine and Subsequent mtMS2 Bioconjugation



concentrations. The precipitation was usually irreversible, likely indicating capsid disassembly and protein unfolding. In some cases, the precipitate could be resolubilized through dilution or dialysis, perhaps indicating that the placement of very hydrophobic ligands, such as **10**, on the exterior surface promotes particle aggregation. While the precipitation could be attenuated by raising the buffer pH somewhat, ultimately the stability of these highly decorated particles limited their characterization and subsequent Gd metalation. Even at lower conversion levels, where less than one of every two monomers was functionalized with aldehyde **2**, the capsids aggregated and precipitated at high concentrations. Thus it was important to perform centrifugal concentration steps carefully. Ultimately, controlling the reaction conditions to append  $\sim 90$  ligands per capsid provided solutions of exterior modified mtMS2 (**11**) that were stable for storage and manipulation, up to approximately 6 mg/mL. Analogous solubility changes were also prominent during Gd chelation.

In stark contrast, internally functionalized capsids (**12**) with high levels of ligand loading could be synthesized and stored at concentrations above 1000  $\mu\text{M}$  (up to 13.7 mg/mL concentrations were evaluated) with no observable precipitation. Although the interior surface could be loaded with as many as 150 bis(HOPO)-TAM ligands, samples labeled to  $\sim 50\%$  monomer functionalization (90 ligands per capsid) were synthesized for comparison to **11**.

For both capsid samples, highly efficient complex formation was achieved by the addition of 1.5 equiv of  $\text{GdCl}_3$  to the capsid conjugates at pH 4.5. After a brief incubation

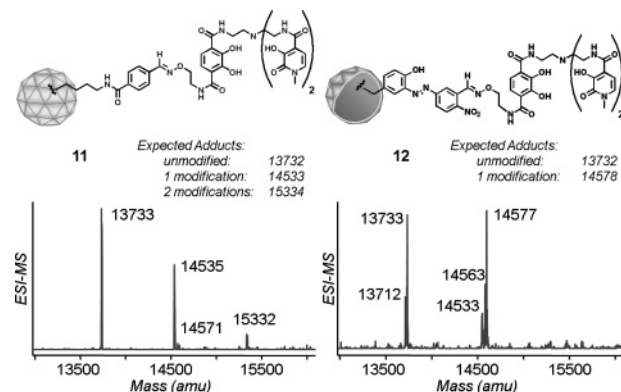
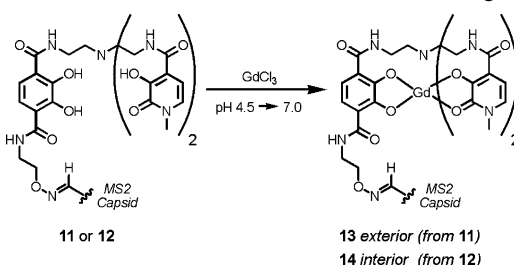


**Figure 2.** Mass spectral characterization of selected MS2-conjugates (see Supporting Information for additional spectra). (left) mtMS2 conjugate **11**. (right) mtMS2 conjugate **12**. The lower mass peaks for each predicted species arise from the elimination of  $\text{H}_2\text{O}$  or  $\text{NH}_3$  molecules during the diazonium coupling reaction.

**Scheme 3.** Formation of mtMS2 MR Contrast Agents<sup>a</sup>



<sup>a</sup> Gd chelation was achieved by the addition of  $\sim 1.5$  equiv of  $\text{GdCl}_3$  to **11** or **12** at pH 4.5. After the pH of each sample was raised to 7.0, free gadolinium was removed by a combination of size-exclusion chromatography, dialysis, and ultrafiltration.

**Table 1.** Comparison of T1 Relaxivities for Contrast Agents

compound	relaxivity per Gd ( $\text{mM}^{-1} \text{s}^{-1}$ )		approximate relaxivity per particle <sup>a</sup> ( $\text{mM}^{-1} \text{s}^{-1}$ )	
	30 MHz	60 MHz	30 MHz	60 MHz
<b>13</b> <sup>b</sup> (exterior)	30.7	23.2	2500	1900
<b>14</b> <sup>b</sup> (interior)	41.6	31.0	3900	2900
<b>15</b> <sup>c</sup> (Gd chelate of <b>10</b> )	5.8	ND	NA	NA

<sup>a</sup> Calculated value: (ionic relaxivity)  $\times$  (number of chelates/capsid).

<sup>b</sup> Determined in 12.5 mM HEPES buffer at pH 6.85 (25  $^\circ\text{C}$ ). <sup>c</sup> Determined in unbuffered  $\text{H}_2\text{O}$  at pH 7.0 (25  $^\circ\text{C}$ ).

(15 min), the pH of each sample was raised to 7.0 by the addition of buffer, Scheme 3. Exhaustive purification of **13** and **14** to remove free gadolinium was achieved using a combination of size-exclusion chromatography, dialysis against citrate buffer, and ultrafiltration centrifugal concentration. Initial determination of the Gd content of the samples was accomplished by inductively coupled plasma atomic emission spectroscopy and was in good agreement with calculated values based on protein concentration and extent of ligand labeling. Gadolinium concentration was also determined by mineralization monitored by relaxometry.<sup>26</sup> The total gadolinium concentrations measured by the two methods agreed to within 10%. Capsid integrity for all mtMS2 conjugates was verified using size-exclusion chromatography and transmission electron microscopy. For



internally labeled samples, these techniques revealed no disassembly or precipitation over a period of months. Incubation of mtMS2 (**1**) control samples with GdCl<sub>3</sub> following the protocol described above showed less than 1.5% of the gadolinium uptake that was observed for **13** and **14** (see Supporting Information).

Following the synthesis and purification of both exterior and interior labeled MS2 MR contrast agents, relaxivities were determined at 30 and 60 MHz, Table 1. Relative to unconjugated chelate **15**, greater than 5-fold enhancement of the ionic relaxivity was observed for both **13** and **14**. Significantly, the ionic relaxivity for MS2 capsids with internal Gd chelates was higher than for those with chelates on the exterior surface, and thus it appears that water diffusion through the capsid was unimpeded. Several factors are likely to contribute to the higher relaxivity for interior Gd chelates. For example, targeting a rigid aromatic tyrosine residue side chain, rather than a more flexible aliphatic lysine side chain, reduces the number of free rotating  $\sigma$ -bonds between the Gd chelate and the capsid surface. We are currently exploring the parameters influencing the difference in relaxivity between all of the paramagnetic agents using nuclear magnetic resonance dispersion (NMRD) spectroscopy.

In summary, we have conjugated high-relaxivity Gd compounds to each surface of bacteriophage MS2. Modification of the interior surface provided high-relaxivity contrast agents that are superior to their exterior counterparts in terms of solubility, stability, and relaxivity. Current efforts are using this masked payload strategy to produce tunable and targetable MR contrast agents for a number of biomedical imaging applications.

**Acknowledgment.** These studies were generously supported by the Biomolecular Materials Program at Lawrence Berkeley National Lab (DE-AC02-05CH11231) and the NIH (GM072700-01 and RO1-HL69832). J.M.H. was supported by a graduate fellowship from the NSF.

**Supporting Information Available:** Detailed experimental procedures for all reactions, purifications, and characterizations are provided. This information is free of charge via the Internet at <http://pubs.acs.org>.

## References

- (1) Allen, M.; Bulte, J. W. M.; Liepold, L.; Basu, G.; Zywicke, H. A.; Frank, J. A.; Young, M.; Douglas, T. *Magn. Reson. Med.* **2005**, *54*, 807–812.
- (2) Anderson, E. A.; Isaacman, S.; Peabody, D. S.; Wang, E. Y.; Canary, J. W.; Kirshenbaum, K. *Nano Lett.* **2006**, *6*, 1160–1164.
- (3) Prasuhn, D. E.; Yeh, R. M.; Obenaus, A.; Manchester, M.; Finn, M. G. *Chem. Commun.* **2007**, 1269–1271.
- (4) Matthews, S. E.; Pouton, C. W.; Threadgill, M. D. *Adv. Drug Delivery Rev.* **1996**, *18*, 219–267.
- (5) Allen, M. J.; Raines, R. T.; Kiessling, L. L. *J. Am. Chem. Soc.* **2006**, *128*, 6534–6535.
- (6) Raatschen, H. J.; Fu, Y. J.; Shames, D. M.; Wendland, M. F.; Brasch, R. C. *Invest. Radiol.* **2006**, *41*, 860–867.
- (7) Kobayashi, H.; Brechbiel, M. W. *Adv. Drug Delivery Rev.* **2005**, *57*, 2271–2286.
- (8) Barrett, T.; Kobayashi, H.; Brechbiel, M.; Choyke, P. L. *Eur. J. Radiol.* **2006**, *60*, 353–366.
- (9) Pierre, V. C.; Botta, M.; Raymond, K. N. *J. Am. Chem. Soc.* **2005**, *127*, 504–505.
- (10) Strijkers, G. J.; Mulder, W. J. M.; van Heeswijk, R. B.; Frederik, P. M.; Bomans, P.; Magusin, P. C. M. M.; Nicolay, K. *Magn. Reson. Mater. Phys.* **2005**, *18*, 186–192.
- (11) For a recent review see: Caravan, P. *Chem. Soc. Rev.* **2006**, *35*, 512–523.
- (12) Schlick, T. L.; Ding, Z. B.; Kovacs, E. W.; Francis, M. B. *J. Am. Chem. Soc.* **2005**, *127*, 3718–3723.
- (13) Kovacs, E. W.; Hooker, J. M.; Romanini, D. W.; Holder, P. G.; Berry, K. E.; Francis, M. B. *Bioconjugate Chem.*, in press.
- (14) Flenniken, M. L.; Liepold, L. O.; Crowley, B. E.; Willits, D. A.; Young, M. J.; Douglas, T. *Chem. Commun.* **2005**, 447–449.
- (15) Flenniken, M. L.; Willits, D. A.; Brumfield, S.; Young, M. J.; Douglas, T. *Nano Lett.* **2003**, *3*, 1573–1576.
- (16) Hooker, J. M.; Kovacs, E. W.; Francis, M. B. *J. Am. Chem. Soc.* **2004**, *126*, 3718–3719.
- (17) Valegard, K.; Liljas, L.; Fridborg, K.; Unge, T. *Nature* **1990**, *345*, 36–41.
- (18) Johnson, H. R.; Hooker, J. M.; Francis, M. B.; Clark, D. S. *Biotechnol. Bioeng.*, available online (Early View).
- (19) Zhang, L. S.; Tam, J. P. *Anal. Biochem.* **1996**, *233*, 87–93.
- (20) Dawson, P. E.; Kent, S. B. H. *Annu. Rev. Biochem.* **2000**, *69*, 923–960.
- (21) Borgia, J. A.; Fields, G. B. *Trends Biotechnol.* **2000**, *18*, 243–251.
- (22) Xu, J.; Franklin, S. J.; Whisenhunt, D. W.; Raymond, K. N. *J. Am. Chem. Soc.* **1995**, *117*, 7245–7246.
- (23) Raymond, K. N.; Pierre, V. C. *Bioconjugate Chem.* **2005**, *16*, 3–8.
- (24) Pierre, V. C.; Botta, M.; Aime, S.; Raymond, K. N. *J. Am. Chem. Soc.* **2006**, *128*, 5344–5345.
- (25) Pierre, V. C.; Botta, M.; Aime, S.; Raymond, K. N. *Inorg. Chem.* **2006**, *45*, 8355–8364.
- (26) Crich, S. G.; Biancone, L.; Cantaluppi, V.; Esposito, D. D. G.; Russo, S.; Camussi, G.; Aime, S. *Magn. Reson. Med.* **2004**, *51*, 938–944.

NL070512C